GEOPHYSICAL RESEARCH LETTERS, VOL. 25, NO.12, PAGES 2123-2126, JUNE 15, 1998

Spatial structure of sprites

Victor P. Pasko, Umran S. Inan, and Timothy F. Bell
STAR Laboratory, Stanford University, Stanford, CA 94305

Abstract. A theory of the electrical breakdown (EB) above thunderstorms is developed. The streamer type of the EB is proposed for the explanation of recent observations of fine spatial structures and bursts of blue optical emissions associated with sprites.

Introduction

Recent sprite observations show optical emissions with highly localized (lateral extents $<\sim$100 m) filamentary structure [e.g., *Sentman et al.*, 1996; *Taylor and Clark*, 1996; *Stanley et al.*, 1996; *Fukunishi et al.*, 1996] and with significant intensity in the blue region of the visible spectrum appearing for $\sim$1 ms during the initial stage of sprite formation [*Armstrong et al.*, 1998; *Suszcynsky et al.*, 1996].

The purpose of this paper is to describe the basic spatial, temporal and optical properties of the EB in different altitude ranges above thunderstorms.

Similarity Laws for Streamer Breakdown

The EB associated with sprites starts in atmospheric regions above thunderstorms where the local electric field (E) exceeds the breakdown field (E_k) following intense lightning discharges [e.g., *Pasko et al.*, 1997, hereafter denoted I]. E_k is the field at which $\nu_i \simeq \nu_a$, where ν_i and ν_a are the ionization and attachment coefficients, respectively [e.g., *Raizer*, 1991, p. 135]. $E>E_k$ ($\nu_i>\nu_a$) and $E<E_k$ ($\nu_i<\nu_a$) correspond respectively to the net creation or removal of electrons. $E>E_k$ is referred to as the overvoltage condition. For small overvoltages, low pressures p and short distances d such that $pd<200$ Torr-cm, the EB proceeds in the form of simple Townsend multiplication of electron avalanches with negligible space charge effects, while for $pd>4000$ Torr-cm the EB may develop in the form of narrow filamentary plasmas (streamers) driven by the highly nonlinear space charge waves [e.g., *Raizer*, 1991, p. 327].

A streamer can develop from an avalanche initiated by a single electron. The initial avalanche phase is followed by the space charge (SC) phase when the SC field E_s associated with polarization of avalanching electrons becomes comparable to the externally applied field [*Vitello et al.*, 1994; *Raizer*, 1991, p. 336]. After the SC phase, the streamer may propagate long distances in the form of a narrow filament. If the initial (prebreakdown) ambient electron density (N_{ae}) is high enough to grow to densities comparable to that in the streamer body, an expansion streamer phase can develop, during which E_s in the streamer head diminishes and the streamer smoothly merges with the growing ambient plasma [*Vitello et al.*, 1993]. An initially large N_{ae} may thus prevent the development of the SC and filamentary phases even if $pd>4000$ Torr-cm.

The conduction current is continuous along the body of the streamer and is equal to the displacement current in the streamer head leading to a relation between streamer characteristics [*Vitello et al.*, 1994]:

$$\frac{R_h}{r_s}\,\frac{v_s \tau_s}{r_s} = \frac{E_b}{E_h} \qquad (1)$$

where R_h is radius of curvature of the streamer head, r_s is the streamer radius (at which the streamer electron density N_s is $1/e$ of its axis value), v_s is the streamer velocity, τ_s the dielectric relaxation time in the streamer body ($\tau_s = \varepsilon_o/\sigma_s$, where σ_s is the conductivity within the streamer), E_h is the peak field in the streamer head, and E_b is the field in the streamer body. Simulation and experimental results agree with (1) under a variety of conditions [e.g., *Dhali and Williams*, 1987; *Vitello et al.*, 1993, 1994; *Grange et al.*, 1995]. Typically $E_b \simeq 0.5E_o$ to $0.9E_o$, where E_o is the ambient E field, and E_h can reach values of up to $5E_k$ to $7E_k$. In general, $10^7 < v_s < 2\times10^8$ cm/s, with lower and upper bounds corresponding to low and high overvoltages, respectively. At ground level, typical values of r_s and N_s are 0.02 cm and 10^{14} cm^{-3}, respectively. For an electron mobility $\mu_e \simeq 4\times10^{-2}$ m^2/V/s (at $E \simeq E_k$) [e.g., I], $\sigma_s = eN_s\mu_e \simeq 0.64$ S/m, and thus $\tau_s \simeq 1.4\times10^{-11}$ s.

For a stably propagating streamer the E field behind the streamer front should relax in time with the same rate as additional ionization is produced. Thus $\tau_s \simeq 1/\nu_{\mathrm{imax}}$, where ν_{imax} is the maximum ionization coefficient realized in the tip of the streamer (corresponding to $E_h \simeq 5E_k$ to $7E_k$). At ground level for $E \simeq 5E_k$ to $7E_k$, $\nu_{\mathrm{imax}} \simeq 10^{11} s^{-1}$ [e.g., I], in agreement with the values of $N_s \simeq 10^{14}$ cm^{-3} and $\tau_s \simeq 1.4\times10^{-11}$ which are typical parameters of stable streamers [e.g., *Dhali and Williams*, 1987; *Vitello et al.*, 1993, 1994; *Grange et al.*, 1995]. For other altitudes, ν_{imax} scales proportionally ($\sim$) with the density of the neutral atmosphere, i.e., $\nu_{\mathrm{imax}} \sim N$ [e.g., I] and thus $\tau_s \sim N^{-1}$. The E_o, E_h and E_b are usually defined with respect to E_k and thus scale in the same way as E_k ($\sim N$). The velocity v_s is closely associated with the electron drift velocity v_d in the body ($v_d = \mu_e E_b$) or in the tip ($v_d = \mu_e E_h$) of the streamer, depending only on the ratio E_o/E_k (i.e., overvoltage). Since $\mu_e \sim N^{-1}$ [e.g., I] and $E_{b,h} \sim N$, v_s remains the same for the same E_o/E_k at different N. Having assumed in (1) that the ratio E_h/E_b as well as R_h/r_s remain the same for the same E_o/E_k ratios at different altitudes (i.e., N) and remembering that $\tau_s \sim N^{-1}$, one can see that (1) can be satisfied at any altitude (any N) if and only if $r_s \sim N^{-1}$. Fig. 1a and 1b respectively illustrate the altitude distributions of τ_s and r_s. Since $N_s = \varepsilon_o/(e\tau_s\mu_e)$ and both μ_e and τ_s are $\sim N^{-1}$, the streamer density scales as $N_s \sim N^2$. In particular, at 0,

Paper number 98GL01242.
0094-8534/98/98GL-01242$05.00

30, 70 and 90 km altitudes we have $r_s \simeq 0.2$ mm, 1.4 cm, 3 m and 83 m; $N_s \simeq 10^{14}, 2\times10^{10}, 5\times10^{5}$ and 6×10^{2} cm^{-3}; $\tau_s \simeq 0.14$ ps, 1 ns, 0.2 μs and 6 μs, respectively. We thus suggest that a unique set of stable streamer characteristics (e.g., r_s, N_s, τ_s) can be specified at each altitude.

To test the similarity laws derived above we numerically simulate negative streamer development (the streamer polarity is defined by the sign of charge in its head) between two plane electrodes with applied steady potentials creating 45% overvoltage field between them. We use a cylindrically symmetric model based on FCT algorothm of *Zalesak* [1979], similar to models previously developed by *Dhali and Williams* [1987] and *Vitello et al.* [1994]. We solve electron and SC continuity and Poisson equations, using the electron mobility, ionization, attachment and optical excitation coefficients derived from kinetic models and swarm experiments [I]. Fig. 2a illustrates streamer development at 0, 30 and 70 km altitudes. Streamers were initiated by placing a cloud of electrons with density N_s (e.g., $N_s=5\times10^{5}$ cm^{-3} at 70 km) and Gaussian spatial distribution with scale r_s (e.g., $r_s=3$ m at 70 km) near the cathode [*Dhali and Williams*, 1987]. Results obtained for ground level are in agreement with previous simulations [*Dhali and Williams*, 1987; *Vitello et al.*, 1994]. At other altitudes the streamers preserve similarity and differ only in spatial and temporal scales.

Fig. 2b (upper panels) illustrates the development of a streamer at 70 km altitude as initiated by a single electron avalanche (a small cloud of electrons with radius 0.25 m and density 5×10^{-3}cm^{-3} was placed near the cathode at t=0). The figure illustrates the moment of transition from the avalanche to SC phase when the SC of avalanching electrons already significantly modifies the ambient E field. The streamer self-consistently reaches radius $r_s \simeq 3$ m as expected for 70 km altitude. Fig. 2b (lower panels) shows a streamer artificially initiated with radius 30 m at 70 km. The streamer appears to be unstable and splits in two narrower filaments. Multistreamer structures were also observed by *Vitello et al.* [1993] for the case of an electrode with curvature significantly exceeding r_s in a point-to-plane discharge gap. Additional tests (not shown) involved artificial wavy perturbations on the initial electron density for the cases shown in Fig. 2a. It appeared that streamers initiated with radius $<r_s$ tend to expand and reach the radius of stable propagation r_s (Fig. 1b), while those with radius $>r_s$ tend to split into narrower filaments.

Sprite Structure at Different Altitudes

The structure of the EB in large volumes associated with sprites ($>10^3$ km^3) depends on N_{ae} at mesospheric altitudes and the time dynamics of the E field. If N_{ae} is large enough, the EB proceeds through collective multiplication of electrons (Townsend mechanism) and the E field is expelled from large volumes of enhanced conductivity. If N_{ae} is low, individual electron avalanches can lead to the formation of individual streamer channels.

Before the postdischarge E field exceeds E_k, it must first attain values just below E_k which correspond to the strong dissociative attachment of electrons. This fact significantly affects the properties of the EB at later times when E exceeds E_k. The characteristic attachment time scale $\tau_a = 1/\nu_{amax}$ (where the maximum attachment coefficient $\nu_{amax} \simeq 7\times10^{7} N/N_o$ 1/s and $N_o=2.7\times10^{19}$ cm^{-3} [e.g., I]) is shown in Fig. 1a. Since $\tau_a \ll 1$ ms (the typical time scale of growth of the E field) at altitudes <80 km, one expects a fast reduction in N_{ae} at these altitudes before the E field exceeds E_k.

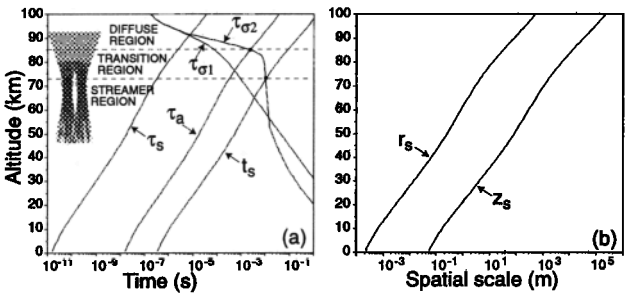

Figure 1. The altitude distribution of different time (a) and spatial (b) scales characterizing the electrical breakdown associated with sprites.

Another important time scale is the ambient dielectric relaxation time $\tau_\sigma = \varepsilon_o/\sigma$, where σ is the ambient conductivity. Fig. 1a shows τ_σ for two model profiles: σ_1 [I] and σ_2 [*Hale*, 1994]. τ_σ determines the persistence of the E field in the conducting atmosphere. Since $\tau_a \ll \tau_{\sigma_2}$ above 85 km, the E field does not persist long enough there to produce any significant attachment.

The third important scale is the time for the development of an individual electron avalanche into a streamer: $t_s = z_s/v_d$, where $z_s = (1/\alpha)\ln(4\pi\varepsilon_o r_s^2 E_k/e)$, is the distance over which the avalanche generates a SC field comparable to the ambient E ($\simeq E_k$), $\alpha=(\nu_i-\nu_a)/v_d$, and the SC is assumed to be concentrated in a sphere with a radius $\simeq r_s$. The logarithm argument scales as N^{-1} so that the product $z_s\alpha$ stays between $\sim$18 to 29, between 0 to 80 km altitude. At the ground, $z_s\alpha \simeq 18$ is the Meek condition for streamer EB [e.g., *Raizer*, 1991, p. 336]. For a 20% overvoltage at ground level, we have $(\nu_i-\nu_a) \simeq 4\times10^{7}$ 1/s, $v_d \simeq 1.6\times10^{5}$ cm/s [I] and $z_s \simeq 5$ cm, in agreement with the criteria on minimum cathode-anode gap size for streamer EB of $pz_s > 4000$ Torr-cm [e.g., *Raizer*, 1991, p. 327]. t_s and z_s are shown in Fig. 1.

Three unique altitude regions are shown in Fig. 1a: (1) The diffuse region (>85 km, $\tau_\sigma < \tau_a$, $\tau_\sigma < t_s$) characterized by collective multiplication of electrons (Townsend mechanism); (2) The transition region (between 75 and 85 km, $\tau_\sigma > \tau_a$, $\tau_\sigma <\sim t_s$) characterized by strong attachment of ambient electrons before the onset of the EB; (3) The streamer region (<75 km, $\tau_\sigma > \tau_a$, $\tau_\sigma > t_s$) also characterized by strong attachment as well as by individual electron avalanches evolving into streamers. Altitudes given above are for the ambient σ_2 and assuming 20% overvoltage in the calculation of t_s and z_s.

The idea of streamer EB as an essential part of sprite development agrees with recent observations of sprite fine structure going well below the video spatial resolution of $<\sim$ 100 m [*Fukunishi et al.*,1996; *Sentman et al.*,1996; *Stanley et al.*, 1996; *Taylor and Clark*, 1996].

Sprite Spectra at Different Altitudes

Most of the results of previous studies [e.g., I] were obtained for ambient σ_1 for which the diffuse region extends down to $\simeq$75 km and transition region down to $\simeq$65 km (Fig. 1a). Optical emissions in the diffusion

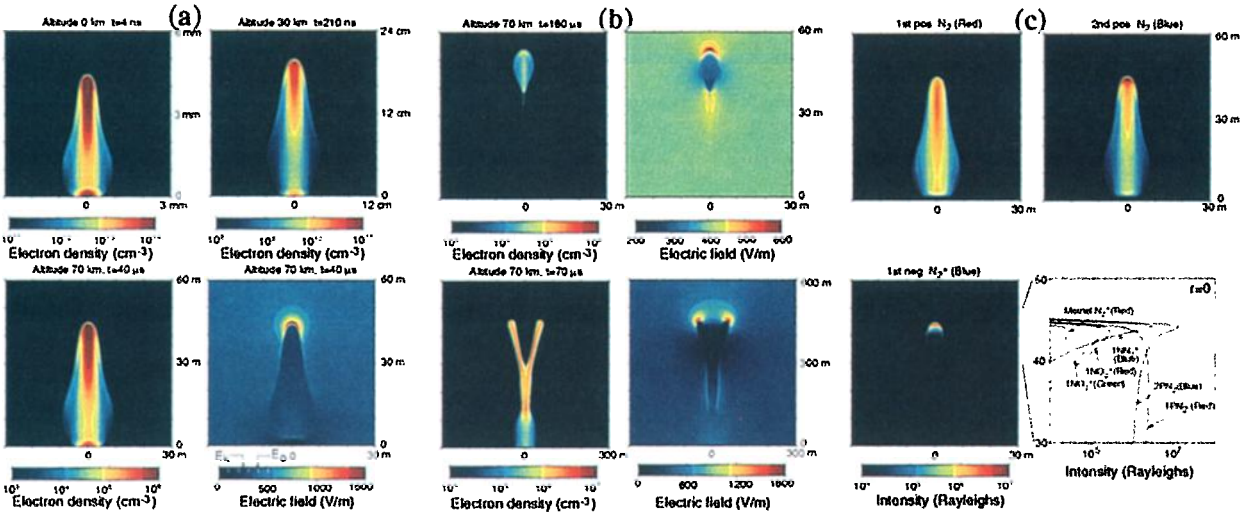

Figure 2. (a) A cross-sectional view of the distribution of the electron density associated with streamer breakdown at 0, 30 and 70 km altitudes. The *lower right* panel shows the E field distribution corresponding to the 70 km case; (b) The streamer development from an individual electron avalanche (*upper panels*), and the splitting of the wide streamer in two narrower filaments (*lower panels*); (c) The intensity of optical emissions in selected bands associated with streamer breakdown at 70 km. The *lower right* panel shows vertical scans of the intensity in the region of the streamer tip.

and transition regions of sprites are dominated by 1st ($1PN_2$) and 2nd ($2PN_2$) positive bands of N_2, with the former being a factor of ~7-8 above the later [I]. The 1st negative ($1NN_2^+$) and Meinel (MN_2^+) bands of N_2^+, and 1st negative band of O_2^+ ($1NO_2^+$) emissions are several orders of magnitude lower than $1PN_2$ and $2PN_2$ [I].

Fig. 2c shows optical emissions associated with streamers formed at 70 km altitude (i.e., typical for the streamer region of sprites). Since E can be $>5E_k$ in narrow regions in streamer tips (Fig. 2a, lower right panel), strong blue emissions from $2PN_2$ and $1NN_2^+$ bands are produced there in a region of $\simeq$5 m vertical extent, well above $1PN_2$ (Fig. 2c). Very low levels of $1PN_2$ at the streamer tip are consistent with the relatively long lifetime of this band (τ_k=6 μs) in comparison with $2PN_2$ (0.5 ns), $1NN_2^+$ (0.7 ns) and τ_s=0.2 μs. $1PN_2$ is dominant in the streamer body at distances $>\tau_k v_s \simeq$6m behind the front, where $v_s \simeq 10^8$ cm/s for the case shown.

The strong blue emissions originating at the streamer tips (e.g., $1NN_2^+$) are produced only in the initial stage of sprite formation during the development of streamers. Recent narrow band photometric measurements and blue video imaging [*Armstrong et al.*,1998; *Suszcynsky et al.*, 1996] showed $\simeq$1 ms bursts of blue optical emissions appearing at the initial stage of sprite formation. The time averaged emissions are dominated by $1PN_2$ (red) band, in agreement with previous observations [*Mende et al.*, 1995; *Hampton et al.*, 1996].

Discussion and Summary

Self-acceleration of electrons. The above analysis is valid for low $E_o<\sim 2E_k$ for which $v_s \leq 2$ km/ms. However, the vertical velocities of sprite development may sometimes be 1/10 of the speed of light (30 km/ms) or even higher [*Fukunishi et al.*, 1996]. It is known that for $E_o>\sim 3E_k$ the streamer is able to generate thermal runaway electrons in its tip which can move in phase with the streamer continuously gaining energy and leading to acceleration (self-acceleration) of the streamer [e.g.,*Babich*, 1982; and references therein]. In laboratory experiments, the self-acceleration manifested itself as measured x-ray radiation believed to be produced from fast electrons with energies greater than the applied voltage (up to hundreds of keV) [e.g.,*Tarasova et al.*, 1974]. The streamer self-acceleration observed in laboratory experiments may well be the same phenomena which is responsible for observed fast upward motions in carrot type sprites with velocities (3-8)$\times 10^4$ km/s [*Fukunishi et al.*, 1996] (corresponding to electrons with energies $\simeq$2-20 keV).

Fig. 3a illustrates the E field in the streamer head for E_o=400 and 600 V/m at 70 km altitude ($\simeq 1.8E_k$ and $2.7E_k$, respectively). For E_o=600 V/m the E field in the tip is almost twice the value $5E_k$, usually defined as the upper bound of applicability of kinetic models used in calculations of ν_i, ν_a, and μ_e [e.g., I]. The average potential drop in the tip exceeds 2 keV (Fig. 3a) and a fraction of electrons [*Gurevich*, 1961] can be accelerated to this energy. The energy estimate is the

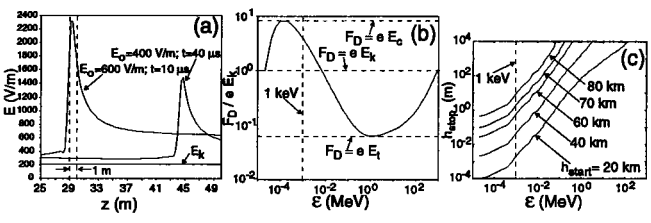

Figure 3. (a) The E field scan at the axis of symmetry (r=0) for the streamer breakdown at 70 km altitude for two E_o values and selected instants of time; (b) The energy distribution of F_D; (c) Stopping distances ($h_{\rm stop}$) of electrons with initial energy ε starting at different altitudes ($h_{\rm start}$) obtained from $\int_0^{\varepsilon} 1/(F_D(\varepsilon)/\rho_{\rm m})d\varepsilon = \int_{h_{\rm start}}^{h_{\rm start}+h_{\rm stop}} \rho_{\rm m}(z)dz$, where $\rho_{\rm m}$ is mass density of air.

same at any altitude since for streamers the E field and length scale respectively as N and N^{-1}. Fig. 3b shows the energy dependence of dynamic friction force of electrons in air F_D (having dimensions of energy/length) normalized by eE_k. F_D combines mass radiative and collision stopping powers [*ICRU Report*, 1984]. Since both F_D and eE_k are $\sim N$, the distribution shown in Fig. 3b is valid for any altitude. The values $E_c \simeq 8E_k$ and $E_t \simeq E_k/15$ shown in Fig. 3b are the critical fields for thermal [*Gurevich et al.*, 1961] and relativistic [*Gurevich et al.*, 1994; *Roussel-Dupre et al.*, 1994] electron runaway, respectively. For $E_o > E_c$ electrons with any initial energy become runaways (e.g., gain more energy from the E field than they lose due to collisions and radiation). In the range $E_t > E_o > E_c$ only those electrons which have initial energy in the region $eE_o > F_D$ become runaways. Cosmic ray secondaries with energies 0.1-1 MeV run away in $E_o \simeq E_t \simeq E_k/15$ field [e.g., *Roussel-Dupre et al.*, 1994], while thermal electrons accelerated in the streamer tips to 2 keV run away in $E_o \simeq 2.5E_k$ (Fig. 3b). For $E_o > 2.5E_k$, electrons which escape from the streamer tips with 2 keV energy remain runaways, avalanching and gaining energy. For $E_o < 2.5E_k$ the electrons lose energy quickly and stop in $\simeq 2$ m at 70 km (Fig. 3c). The self-acceleration may contribute to additional gain of energy and runaway at lower E_o fields.

Heating of neutral gas. The rate of change of neutral temperature due to electron-neutral collisions in the streamer channel is $dT/dt \simeq \delta \nu_{\text{eff}} T_e N_s/N$, where T_e is the temperature of electrons (assumed to be $\simeq 1$ eV), $\delta \simeq 5 \times 10^{-3}$ is the fraction of electron energy lost in one collision, $\nu_{\text{eff}} = e/(m_e \mu_e) = 4.4 \times 10^{12} N/N_o$ 1/s, and $N_s = 10^{14} N^2/N_o^2$ cm^{-3}. dT/dt can be expressed as: $dT/dt = 8.8 \times 10^8 N^2/N_o^2$ °K/s. For times $t_s = 3 \times 10^{-7}$ s ($z_s = 5$ cm) of streamer formation at the ground, $\Delta T = 264$°K, while for a streamer with length $\simeq 1$ m, $\Delta T = 5280$ °K, fully sufficient for the streamer to leader transition [*Raizer*, 1991, p. 365]. Due to the strong heating of the neutral gas in the streamer channel and associated thermal ionization for gaps >1 m at the ground, discharge always proceeds in the form of leader [*Raizer*, 1991, p. 366]. Although 1 m scales to 1-5 km at lower sprite altitudes 50-60 km, the heating of the neutrals on the time scale of sprites (10 ms) $\Delta T/T \simeq 2$-0.2% appears to be unimportant. Sprites thus manifest themselves in the streamer (not leader) type discharge at lower altitudes (in the streamer and transition regions) and glow discharge at higher altitudes (in the diffuse region).

In summary, we have developed a theory describing basic properties of the EB above thunderstorms which appears to be consistent with some sprite characteristics observed experimentally (e.g., fine structure and bursts of blue emissions). No detailed comparisons with particular sprites are attempted since the data obtained to date is not yet of sufficient spatial and temporal resolution to make such comparisons, and the theory itself is not yet of sufficient detail to explain all of the extremely rich morphological features of sprites observed to date.

Acknowledgments. This work was sponsored by NASA NAGW5-6264 and NSF ATM-9522816 grants to Stanford University.

References

Armstrong R.A., J. A. Shorter, M. J. Taylor, D. M. Suszcynsky, W. A. Lyons, and L. S. Jeong, Photometric measurements in the SPRITES' 95 and 96 campaigns of nitrogen second positive (399.8 nm) and first negative (427.8 nm) emission, *J. Atmos. Terr. Phys., in press*, 1997.

Babich, L.P., A new type of ionization wave and the mechanism of polarization self-acceleration of electrons in gas discharge at high overvoltages, *Sov.Phys.Dokl., 27*,215,1982.

Dhali, S.K., and P. F. Williams, Two-dimensional studies of streamers in gases, *J. Appl. Phys., 62*, 4696, 1987.

Fukunishi, H., Y. Takahashi, M. Fujito, Y. Watanabe, S. Sakanoi, Fast imaging of elves and sprites using a framing/streak camera and a multi-anodo array photometer, *EOS Trans. AGU, 77*, Fall Meet. Suppl., F60, 1996.

Grange, F., N. Soulem, J. F. Loiseau, and N. Spyrou, Numerical and experimental determination of ionizing front velocity in a DC point-to-plane corona discharge, *J. Phys. D: Appl. Phys., 28*, 1619, 1995.

Gurevich, A. V., On the theory of runaway electrons, *Sov. Phys. JETP, 12*, 904, 1961.

Gurevich,A.V.,G.M.Milikh,and R.A.Roussel-Dupre,Nonuniform runaway air-breakdown, *Phys.Lett.A, 187*, 197, 1994.

Hampton,D.L.,M.J.Heavner,E.M.Wescott,and D.D.Sentman, Optical spectra of sprites, *Geophys.Res.Lett., 22*, 89,1995.

International Commission on Radiation Units and Measurements, Stopping powers for electrons and positrons, tables 8.1 and 12.4, ICRU Rep. 37, Bethesda, Md., 1984.

Mende, S. B., R. L. Rairden, and G. R. Swenson, and W. A. Lyons, Sprite spectra: N_2 1 PG band identification, *Geophys. Res. Lett.,22*, 3468, 1995.

Pasko, V.P., U.S.Inan, T.F.Bell, and Y.N.Taranenko, Sprites produced by quasi-electrostatic heating and ionization in the lower ionosphere, *J.Geophys.Res., 102*, 4529, 1997.

Raizer, Y. P., *Gas discharge physics*, Springer-Verlag Berlin Heiddelberg, 1991.

Roussel-Dupre, R. A., A. V. Gurevich, T. Tunnel, and G. M. Milikh, Kinetic theory of runaway breakdown, *Phys. Rev., 49*, 2257, 1994.

Sentman, D. D., E. M. Wescott, M. J. Heavner, and, D. R. Moudry, Observations of sprite beads and balls, *EOS Trans. AGU, 77*, Fall Meet. Suppl., F61, 1996.

Stanley, M., P. Krehbiel, W. Rison, C. Moore, M. Brook, and O. H. Vaughan, Observations of sprites and jets from langmuir laboratory, New Mexico, *EOS Trans. AGU, 77*, Fall Meet. Suppl., F69, 1996.

Suszcynsky D. M., R. Roussel-Dupre, H. DeHaven, E. Symbalisty, S. Voss, W. Lyons, and T. Nelson, Blue-light imagery and photometry of sprites, *EOS Trans. AGU, 77*, Fall Meet. Suppl., F69, 1996.

Tarasova,L.V.,L.N.Khudyakova,T.V.Loiko,and V.A.Tsukerman,Fast electrons and x rays from nanosecond gas discharges at 0.1-760 torr, *Sov.Phys.Tech.Phys., 19*,351, 1974.

Taylor, M.J., and S. Clark, High resolution CCD and video imaging of sprites and elves in the N_2 first positive band emission, *EOS Trans.AGU,77*, Fall Meet.Suppl.,F60, 1996.

Vitello, P.A.,B.M.Penetrante,and J.N.Berdsley,Multi-dimensional modeling of the dynamic morphology of streamer coronas, in *Non-Thermal Plasma Techniques for Pollution Control*, NATO ASI Series,Vol.G34, Part A, p.249, 1993.

Vitello, P. A., B. M. Penetrante, and J. N. Bardsley, Simulation of negative-streamer dynamics in nitrogen, *Phys. Rev. E, 49*, 5574, 1994.

Zalesak, S.T., Fully multidimensional flux-corrected transport algorithms for fluids, *J.Comput.Phys., 31*, 335, 1979.

V. P. Pasko, U. S. Inan, T. F. Bell, STAR Laboratory, Stanford University, Stanford, CA 94305.

(Received February 9, 1998; revised March 25, 1998; accepted March 30, 1998.)